NASA CONTRACTOR REPORT

RADIATION DAMAGE IN SILICON

PREPARED BY: N. ALMELEH, B. GOLDSTEIN (Project Engineer),
Y. SHAHAM, AND J. J. WYSOCKI

APPROVED BY: P. RAPPAPORT

FIRST SEMIANNUAL REPORT
FOR THE PERIOD
OCTOBER 15, 1963 TO APRIL 15, 1964

Prepared under Contract No. NAS 5-3788

RADIO CORPORATION OF AMERICA
RCA LABORATORIES
PRINCETON, NEW JERSEY

for

NATIONAL AERONAUTICS & SPACE ADMINISTRATION • GREENBELT, MD. • MAY 1964
GODDARD SPACE FLIGHT CENTER

NASA CONTRACTOR REPORT

RADIATION DAMAGE IN SILICON

PREPARED BY: N. ALMELEH, B. GOLDSTEIN (Project Engineer),
Y. SHAHAM, AND J. J. WYSOCKI

APPROVED BY: P. RAPPAPORT

FIRST SEMIANNUAL REPORT

FOR THE PERIOD

OCTOBER 15, 1963 TO APRIL 15, 1964

Prepared under Contract No. NAS 5-3788

RADIO CORPORATION OF AMERICA
RCA LABORATORIES
PRINCETON, NEW JERSEY

for

NATIONAL AERONAUTICS & SPACE ADMINISTRATION • GREENBELT, MD. • MAY 1964
GODDARD SPACE FLIGHT CENTER

19886

ABSTRACT

19886

Electron paramagnetic resonance studies at 27°K of a newly observed center in electron-irradiated p-type silicon have yielded the following information. The principal axes are <221>, <1$\bar{1}$0>, and <11$\bar{4}$> with respective g-values of 2.0000, 2.0066, and 2.0056. This center is definitely different from the J-center and a recently reported aluminum center. Preliminary measurements of introduction rates at various bombardment energies are 0.25 cm^{-1} at 6.6 MeV, 0.22 cm^{-1} at 5.5 MeV, and 0.15 cm^{-1} at 3.0 MeV. So far, this center is found only in silicon which contains oxygen in concentrations $\geq 10^{18}/cm^3$. These data, together with optical and electrical measurements of others, lead us to suggest that this new defect be identified with a level about 0.3 eV above the valence band and be associated with substitutional oxygen and a next-nearest-neighbor silicon interstitial.

Studies of the effects of impurities on radiation characteristics in silicon have begun. These include diffusion length measurements using surface-barrier diodes and EPR measurements of lithium-doped silicon. Techniques have been successfully applied to the fabrication of the diodes and to lithium doping of the silicon. The paramagnetic resonance due to lithium has been observed at 27°K. It consists of one narrow line with a g-value of 1.9997.

Bombardment-induced changes in the photovoltaic parameters of Si p/n, Si n/p, and GaAs p/n solar cells were measured for protons with energies in the range 185 to 545 keV. In the GaAs cell, the short-circuit current changed most during irradiation, while in both types of Si cells the shape of the I-V characteristic and the open-circuit voltage were more sensitive to radiation than the short-circuit current. The rate of change of these parameters per incident particle increases with proton energy. In terms of long-term radiation susceptibility, the cells can be listed in the following order: GaAs chromium-treated cells, GaAs standard cells, Si n/p and finally Si p/n cells. These results can be explained in terms of the thickness of the damaged region, and the junction depth. The results of this experiment also help explain Relay and ANNA 1B experiments with unshielded solar cells where the short-circuit current dropped rapidly with time. It is clear that both GaAs and Si cells will require minimum thickness shields in low-energy proton environments.

Authors

TABLE OF CONTENTS

LIST OF ILLUSTRATIONS

I. INTRODUCTION

This report is divided into three parts. The first describes the EPR work which has been done on a newly observed paramagnetic center first reported in the Final Report under Contract No. NAS 5-457. This includes some preliminary measurements of the defect introduction rate at different bombarding energies, the characteristic g-values in the principal directions, and a brief discussion of the identification of the center. The second part describes the work which was recently begun, aimed at studying the possible effects of certain impurities on the radiation damage properties of silicon. This work includes measurements of diffusion length, and changes in the EPR spectrum of the impurity and/or the radiation-induced defect. The third section presents a detailed report of low-energy proton bombardment of silicon and gallium arsenide solar cells. The analysis of this work has been only recently completed and the results may be of considerable significance in understanding some of the recent satellite experiments on solar cells.

II. MEASUREMENTS ON A NEWLY OBSERVED PARAMAGNETIC CENTER IN IRRADIATED p-TYPE SILICON

The nature of lattice defects in semiconductors, produced by irradiation, has been the subject of a considerable amount of experimental study over the past few years. Much that has been learned about these defects has been obtained by measurements such as resistivity, minority-carrier lifetime, and optical absorption. However, specific knowledge concerning the identity of the defect in its immediate crystal environment has so far been obtained only through electron spin resonance investigations. The combination of electron spin resonance together with the other experimental methods mentioned above is by far the most fruitful approach to understanding the complete physical character of radiation damage centers.

In a previous report,* the crystal symmetry properties for a new center in p-type silicon, introduced by electron irradiation, were discussed in detail from the data obtained by electron spin resonance measurement. As part of the effort to further characterize the center, a program has been set up to study the spin concentration of this center as a function of a) the flux for a given bombardment energy, b) the location of the Fermi level, and c) the specific p-type dopant impurity. In addition, optical absorption and photoconductivity measurements are planned to supplement the information obtained from electron spin resonance and solar cell measurements.

A. EXPERIMENTAL SECTION

1. Apparatus

The EPR spectrometer* is essentially a 23-Gc superheterodyne microwave bridge with a Varian V4500 EPR system. During the past six months, several improvements have been made on this equipment. The bridge has been completely rebuilt with components of greater precision. A new, shorter sample arm was designed which incorporates several important features (see Fig. 1), the most important of which is an adjustable coupling from the waveguide to the cavity. This enables us to obtain maximum sensitivity for different samples as discussed by Feher[1] and Gordon.[2] It also simplifies the control of the chosen mode of operation, i.e., either dispersion or absorption, by changing the phase at the reference arm of the microwave bridge. Provision has also been made for applying stress to the sample. The cavity has been changed and is now made from gold-plated Hysol plastic to minimize noise due to eddy current in the walls. The cavity and the coupling have been enclosed in a thin-walled brass can which prevents leaks into the system, thus eliminating another source of noise and frequency drifts. All the control rods are brought out at the top through Veeco vacuum "quick-chucks".

The net effect of these modifications has been to increase significantly both the overall stability and the sensitivity of the equipment – the latter by a factor of at least five.

* See Final Report, Contract No. NAS 5-457.

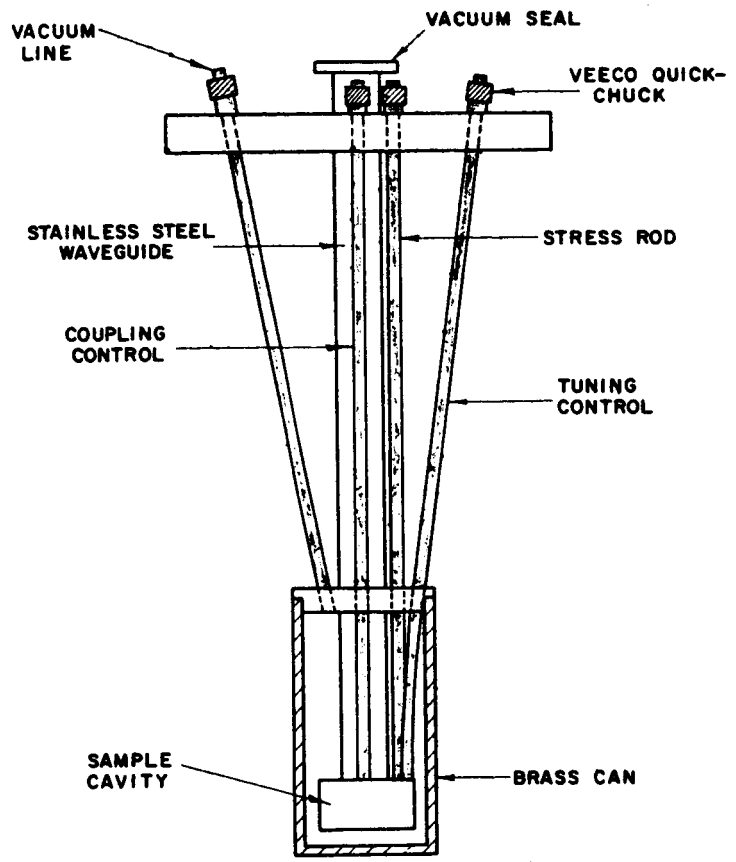

Fig. 1. Schematic representation of sample cavity and controls.

2. Irradiations

Several electron irradiations were performed (and continue to be performed) at various energies and fluxes. A 700-keV irradiation and a 1-MeV irradiation were done at RCA's Van de Graaff accelerator. A 3-MeV irradiation was made at Electronized Corp. Burlington, Mass., while 5.5-MeV and 6.6-MeV irradiations were made at the Ethicon Co., Somerville, N.J., using their linear accelerator. The irradiations were performed at room temperature (maximum temperature rise to 70°C) with the samples mounted on water-cooled copper blocks. Electron fluxes ranged from 1×10^{16} el/cm^2 to 4×10^{17} el/cm^2. The standard sample size was $0.095 \times 0.290 \times 0.025$ inches. For a thickness of 25 mils only the low-energy irradiations at 1 MeV and 700 keV resulted in nonuniform energy absorption in the sample. At higher energies, absorption was homogeneous throughout the sample.

3. Experimental Results

Part of the difficulty in determining the introduction rates of the new paramagnetic center stems from the saturation of the resonance lines at moderate klystron power levels. This situation has been improved, in part, by the increased sensitivity of the spectrometer resulting

from the modifications described above, so that even lower klystron power levels can be used. To completely eliminate the saturation effect in the spin concentration determination, it was necessary to measure a reference sample of known spins* simultaneously with the irradiated silicon sample as a function of klystron power level. Since it is known that the silicon conduction electron line does not saturate, comparison of the spectra of the two samples lets us know precisely when the saturation effect enters into the measurement. In this way, we were able to calculate the absolute concentration of the defect centers and in turn make some preliminary estimates of the introduction rates at various bombardment energies.

Introduction rates of 0.25 cm^{-1}, 0.22 cm^{-1}, and 0.15 cm^{-1} were obtained for the new center at irradiation energies of 6.6 MeV, 5.5 MeV, and 3.0 MeV, respectively. These results are preliminary since at this time only two samples have been bombarded at each of these energies at fluxes of 5×10^{16} el/cm^2 and 2×10^{17} el/cm^2. It is planned to run samples throughout the range of fluxes from 1×10^{16} to 5×10^{17} el/cm^2 to determine the dependence of the production rate of these centers on flux and energy.

In the course of studying the effect of bombardment energies on the production of the new center an interesting dependence of the "J"-center was observed. The J-center is detected in our experiments in addition to the new center. This is shown in Fig. 2, for which the silicon sample was irradiated at 1 MeV at a flux of 2×10^{17} el/cm^2. As the bombardment energy was

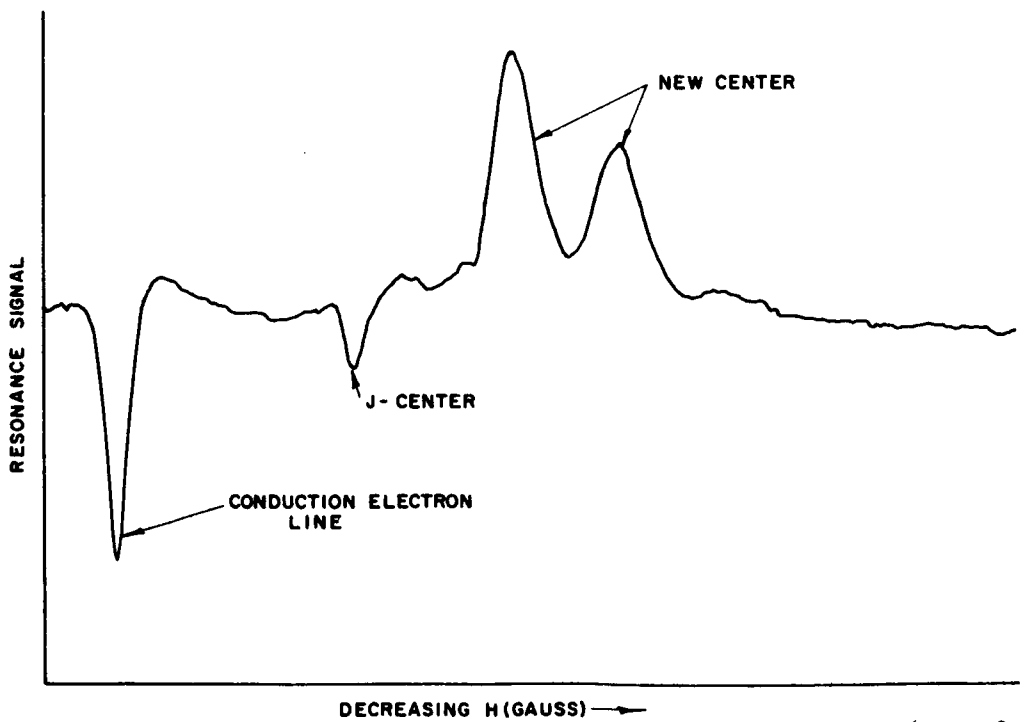

Fig. 2. EPR spectrum of irradiated silicon. E = 3 MeV, $\phi = 4 \times 10^{16}$ μ/cm^2, $H \perp <100>$, T = 27°K.

* For this purpose, the resonance line due to conduction electrons in silicon is used. The electron concentration is independently determined.

increased to 5.5 MeV and finally to 6.6 MeV, the J-center resonance decreased and ultimately disappeared. This has been observed recently and bears further investigation in connection with the growth of the new center.

Another interesting feature of the new center is that its presence is discernible only in silicon containing oxygen (concentration $\sim 10^{18}/cm^3$). In a float zone silicon sample having an oxygen content less than $10^{16}/cm^3$ and which has been irradiated at 1 MeV at a flux of 5×10^{16} el/cm^2, only the J-center appears. The density of the J-center is unaffected by the change of nearly two orders of magnitude in oxygen concentration in contrast to its effect on the new center. The fact that the new center appears to be related in some way to the presence of oxygen should be of value in determining the physical properties of the center.

B. DISCUSSION

Until now, there have been only two paramagnetic centers reported for electron-irradiated p-type silicon. One is the J-center and the other is a recently reported center specifically associated with aluminum.[3] Both have been studied extensively by Watkins.[3,4] We have now definitely established that the *new* center is different from both the J-center and the aluminum centers. Table I shows that the new center and the J-center have different principal axes and g-values; furthermore, the new center has been seen in both gallium- and boron-doped silicon, thus dissociating it from the aluminum resonance.

TABLE I

PRINCIPAL AXES AND g-VALUES FOR THE J-CENTER AND THE NEW CENTER

	g-VALUE	PRINCIPAL AXES
New Center	2.0000	$< 221 >$
	2.0066	$< 1\bar{1}0 >$
	2.0056	$< 11\bar{4} >$
J-Center	2.0004	$< 11\bar{1} >$
	2.0020	$< 011 >$
	2.0041	$< 2\bar{1}1 >$

It is worthwhile at this time to summarize some of the pertinent measurements of resistivity, minority-carrier lifetime, and photoconductivity currently available on electron-irradiated p-type silicon so that we can briefly discuss the new defect center. Studies of the recombination properties of bombardment-induced defects in silicon by Wertheim[5] disclose the existence of three defect levels within the forbidden gap lying at (E_c – 0.16 eV), (E_c – 0.4 eV), and at

(E_v + 0.27 eV). The level at (E_c – 0.16 eV) has been identified by Watkins[6] using electron spin resonance, as the A center and the (E_c – 0.4 eV) level with the B, C and E centers. Hill,[7] measuring carrier removal rates in p-type silicon, finds levels located at 0.3 eV and 0.05 eV above the valence band, the dominant level being the one at 0.3 eV. More recently, Vavilov[8] has also found, by measuring the spectral response of photoconductivity, that electron bombardment produces a level at 0.3 eV. He finds, in addition, that the 0.3-eV level appears only in silicon which contains oxygen.

Our preliminary measurements of the introduction rates for the new center are close to the values obtained by Hill for the level lying at 0.3 eV. In addition, the fact that the new center and the level at 0.3 eV are detected only in silicon containing oxygen leads us to suggest that the level at (E_v + 0.3 eV) is in fact the level to be associated with the paramagnetic center reported here. Since its symmetry direction < 221 > is from a lattice site to a next-nearest neighbor interstitial, it is also tentatively suggested that the center involves a substitutional oxygen atom associated with an interstitial silicon atom.

Additional experiments are required to explore further the connection between the 0.3-eV level and the new defect center. They include more complete and detailed introduction rate measurements and optical absorption measurements. These experiments are in progress and will be the chief basis of our future studies.

III. EFFECTS OF IMPURITIES ON RADIATION DAMAGE IN SILICON

A. DIFFUSION LENGTH STUDIES

1. Introduction

Diffusion length measurements are being made to assess the effects of impurities in silicon on its radiation behavior. The measurement is based on the electron-voltaic effect generated by 1-MeV electrons in surface-barrier diodes. The use of this effect to obtain the diffusion length has been covered in the literature.[9] The incident electrons, in losing energy in the material, generate electron-hole pairs at the expense of 3.6 eV per pair. If a junction or other space-charge dipole is present, some of these pairs are separated, resulting in a short-circuit current I_{sc}. The ratio of I_{sc} to the incident electron current I_B (which we shall call the multiplication m) is directly proportional to the sum of the diffusion lengths on both sides of the junction if the pairs are produced uniformly throughout the material. Generally, an Al absorber is used to bring m close to its maximum value where the rate of change with absorber thickness is zero.

The parameter used to measure the effect of impurities will be the diffusion-length-flux constant K obtained from

$$1/L^2 = 1/L_o^2 + K\,\phi \tag{1}$$

where L is the diffusion length with initial value L_o. The constant K is associated with the defect in question through

$$K = N_r \sigma f v/D \tag{2}$$

where N_r is the defect introduction rate, σ is the capture cross section, f is the Fermi filling factor, v is the minority-carrier's thermal velocity, and D is its diffusion constant. The diodes, made from silicon doped with different impurities, are to be irradiated to various flux levels with periodic measurements of L. From this, K can be determined and so related to the particular impurity in the silicon.

A surface-barrier junction will be used rather than a p-n junction. This has the advantage of not requiring high-temperature processing. Other advantages are the ease of fabrication and simplicity of the final device. This study is primarily interested in the effect of impurities on diffusion length. Ultimately, the results will be applied to solar cells where processing will have to be taken into account.

2. Experimental Results

Diodes are being fabricated by the same technique used for surface-barrier particle detectors.[10] Electroless Ni and evaporated Al are used for the ohmic and rectifying contacts, respectively, to p-type Si. Preliminary radiation measurements on several units of this type have been made, and the feasibility of the approach verified.

The multiplication curve for a diffused solar cell has also been measured as a function of Al absorber thickness to establish the constant relating the multiplication, m, to the diffusion length, L, which will be called the specific ionization S, i.e., S = m/L. This measurement also establishes the absorber thickness for maximum output. A value of 258 pairs/μ has been obtained for an absorber thickness of 14 mils of Al. This value of specific ionization includes a 3 percent backscatter correction, as well as a 4 percent Z/A correction to convert the Al thickness to Si thickness.

B. ELECTRON PARAMAGNETIC RESONANCE STUDIES

The interaction between impurities and paramagnetic defects can be directly detected by measuring changes in the EPR spectrum of the impurity and/or the defect center. Accordingly, to use this effect a fast-diffusing, paramagnetic impurity (lithium) has been chosen for experiments involving the dominant paramagnetic defects produced by electron bombardment. These are the C-center in n-type silicon and its counterpart, the J-center in p-type silicon. The planned experiments are to bombard lithium-diffused silicon and to diffuse lithium into bombarded silicon. Ultimately, it is hoped to correlate some of the results of these experiments with those involving the diffusion length experiments mentioned in the preceding paragraphs.

Lithium-doped silicon has been prepared by diffusing the lithium into the silicon at 300°C from an oil suspension. This produces n-type silicon with a resistivity of from 0.1 to 0.3 Ω-cm. Higher temperature diffusions produce much lower resistivities in the range 0.005 to 0.05 Ω-cm. These resistivities are not suitable for EPR work since they load the r-f cavity. Diffusions much below 300°C produce spotty p, n, and indeterminate regions in the silicon. The EPR spectrum of lithium in silicon has been observed by comparing it with heat-treated "blanks". The spectrum consists of one narrow line, about 2 gauss in half-width, with an isotropic g-value of 1.9997. "Oxygen-free" silicon (i.e., oxygen content $< 10^{16}/cm^3$) gives a much smaller lithium resonance than that of silicon containing about $10^{18}/cm^3$ oxygen atoms.

IV. LOW-ENERGY PROTON BOMBARDMENT OF SILICON AND GALLIUM ARSENIDE SOLAR CELLS

A. INTRODUCTION

An experiment on the Relay I satellite has shown that uncovered GaAs and Si solar cells degrade rapidly in outer space. In one day, the short-circuit current of the GaAs, Si p/n and Si n/p cells degraded by 50, 60 and 38%, respectively.[11] Terrestial experiments with high-energy particles, as well as experiments on Explorer XII and ANNA 1-B satellites, suggested that the Relay results were caused by low-energy protons.[12-14] Explorer XII showed that a substantial number of protons with energies below 3 MeV existed in outer space.[12] Further evidence was obtained from CdS counters on the Injun I satellite which detected a large number of protons and/or ions with energies in the 100-keV range.[15] Assuming that these particles are protons with an average energy of 100 keV, Freeman computed an intensity of 3×10^8 protons/cm^2 sec sterad or an omnidirectional flux of 3.8×10^9 p/cm^2 sec.[15] In view of the space results and the lack of information on the effects of low-energy protons on solar cells, two experiments were performed in which Si and GaAs cells were irradiated with 185-to 545-keV protons.[16] These experiments used the Van de Graaf proton generator at Brown University.

Table II shows the range of low-energy protons in Si and GaAs. Because the range is small, defects will be introduced close to the surface. Therefore, the junction depth and thickness of the antireflection coating become important parameters in the observed behavior. The

TABLE II

RANGE OF LOW-ENERGY PROTONS [17]

PROTON ENERGY (keV)	RANGE (μ)	
	Si	GaAs
185	1.8	0.9
325	3.6	1.9
450	5.6	2.8
530	6.8	3.5

These values are for normal incidence. For bombardments at 45°, the effective penetration is obtained by multiplying these values by 0.707.

short-circuit current of GaAs cells, which depends upon the collection of carriers generated within 2 microns of the surface, is expected to be extremely susceptible to low-energy protons. Since the surface regions contribute only about 20 percent to the short-circuit current of Si cells, however, these cells should be more resistant to low-energy protons, at least as far as the short-circuit current is concerned.[18]

B. 185-keV TO 545-keV PROTON EXPERIMENT II

This discussion of experimental details refers to a run made in December, 1963, (hereafter called experiment II) since it was more extensive and complete than the one in February 1963 (experiment I). However, the conduct of both experiments was generally the same.

The GaAs and Si cells were cut into 1 cm × 0.6 cm pieces and soldered to ceramic discs. A GaAs, Si p/n and Si n/p cell were mounted side-by-side on most of the discs to ensure reliable data on the relative performance of these cells. The initial properties of the cells are listed in Table III, together with the standard deviation σ. The cells were obtained as follows: PH-Heliotik; T – IRC; R – Hoffman; MT – RCA Mountaintop; MR – RCA Mountaintop, Relay-type; G, SG, and SCR-RCA Somerville. (The SCR cells were specially treated during fabrication.) The diffusion lengths L_o were measured as described in the literature.[9] The range in the junction depths indicates the variation observed in the cells sectioned. The final column of Table III indicates the experiment in which the cells were irradiated.

TABLE III

INITIAL PROPERTIES OF CELLS USED FOR 185-545 keV PROTON BOMBARDMENT

TYPE	NO. OF CELLS	SUNLIGHT EFFICIENCY $\eta_o \pm \sigma$	$L_o \pm \sigma$ (μ)	JUNCTION[9] DEPTH (μ)	EXPERIMENT
Si p/n PH	4	11.5 ± 0.9	–	–	I
T	31	6.5 ± 0.9	131 ± 37	–	II
R	2	9.9 ± 0.3	–	–	II
Si n/p MT	4	10.4 ± 0.4	–	(0.39 – 0.60)	I
MR	40	10.5 ± 1.3	152 ± 21	(0.22 – 0.38)	II
GaAs G	4	10 ± 0.3	–	1.1 – 1.3	I
SG	7	7.6 ± 0.9	2.1 ± 0.1*	0.41	II
SCR	9	8.5 ± 0.9	1.5 ± 0.2*	0.36	II

* Assuming 3.6 eV are required to generate an electron-hole pair.

The discs were mounted on a water-cooled block at an angle of 45° to the proton beam, and the cells were irradiated in a vacuum of approximately 10^{-5} torr. The photo-characteristic of the cells was measured periodically while the beam was intercepted with a shutter. The light source used was an incandescent projection lamp filtered by 2 inches of water.

1. Flux Measurements

The incident flux was measured with a collector consisting of three cups, one within the other. This collector was used throughout the run; the 45° block holding the cells was located to one side of the cup opening. The use of three nested cups for a collector was required to obtain

reliable readings of the small beam currents used ($\sim 10^{-10}$ amps). In experiment I, beam-current readings obtained with a standard Faraday cup could be either positive or negative. The negative values were attributed to a secondary electron component generated when the protons bombarded the cup face.

In the three-cup arrangement, the outer cup was grounded; the second was biased to repel electrons; and the innermost cup collected the incident protons. The flux incident on the cells was given by the cup current divided by the area of the limiting aperture, assuming a uniform beam distribution. A nearly uniform beam distribution over the cup and cell areas was ensured by defocussing the beam and deflecting it vertically and horizontally by means of incommensurate, periodic sawtooth signals. Subsequent measurement showed that the beam distribution was uniform to within 20% over the area occupied by the cells.

2. Photovoltaic Response

a. Si p/n Cells – The changes in the open-circuit voltage V_o, short-circuit current I_s, and maximum power output P_m of the IRC(T) and Hoffman (R) cells measured with the incandescent light source mentioned above are shown in Figs. 3 through 6. The fractional open-circuit voltage V_o remaining after bombardment is shown in Fig. 3. The 450-keV protons are more effective in reducing the voltage than 185-keV protons for the T cells while 450- and 530-keV protons are equivalent in degrading the voltage of the R cells. Further, the R cells are two orders of magnitude more sensitive than the T cells to 450-keV protons. The parameter which is believed to explain this difference in sensitivity is a shallower junction depth in the R cells.

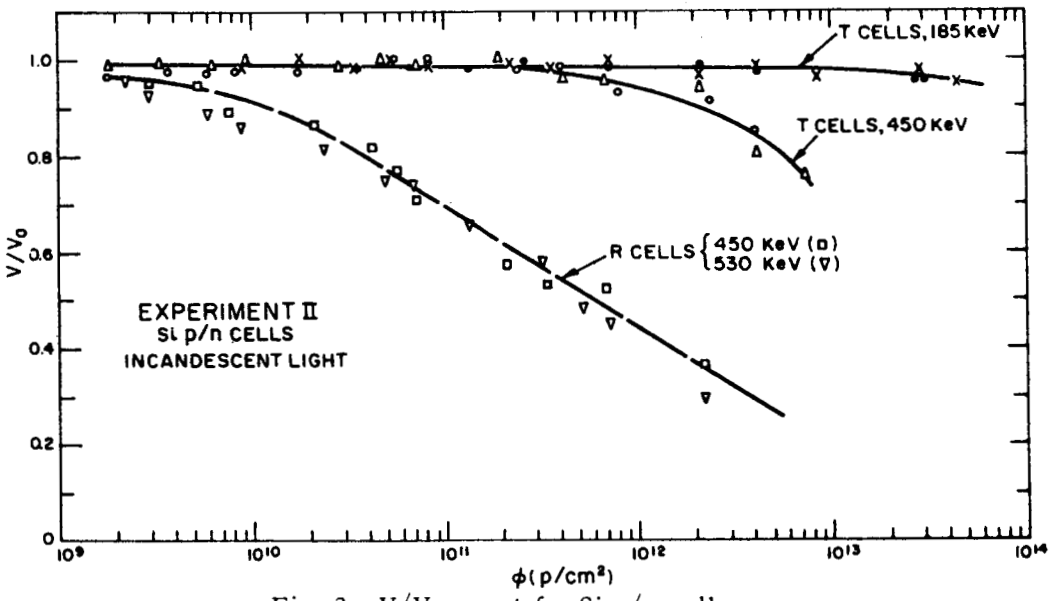

Fig. 3. V/V_o vs. ϕ for Si p/n cells.

Figure 4 shows the fractional short-circuit current remaining after a given flux. The energetic protons cause a more rapid decrease for both types of cells. However, the R cells decay 20 to 40 times more rapidly when bombarded by 450-keV protons than the T cells, again because of their shallower junction depth. Furthermore, the R curves show a faster fall-off (~ 25%/decade).

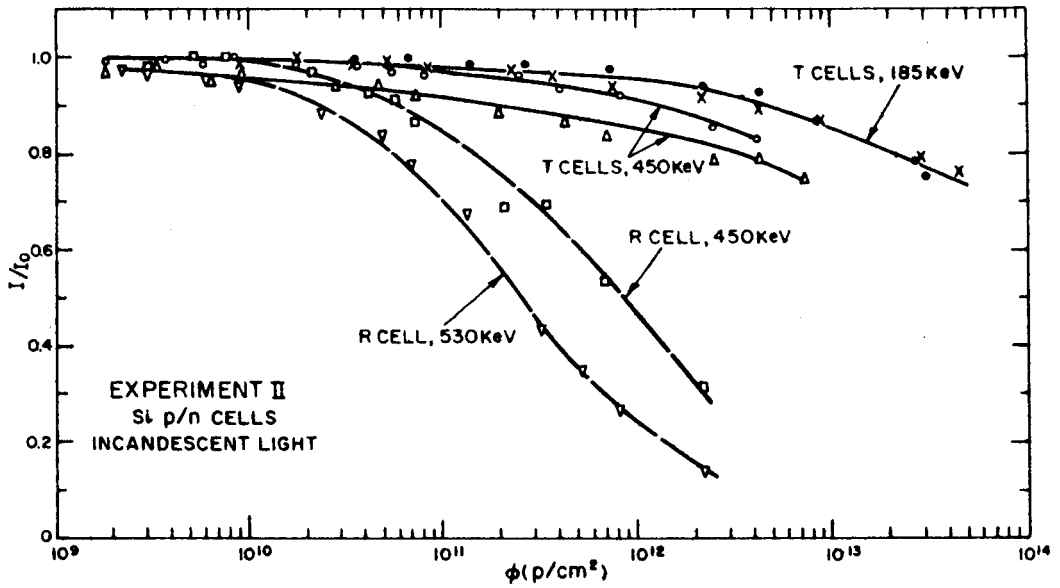

Fig. 4. I/I_o vs. ϕ for Si p/n cells.

Figure 5 shows the fractional remaining maximum power as a function of flux. Similar comments apply as above except that the ratio of degradation rates of the R and T cells for 450-keV

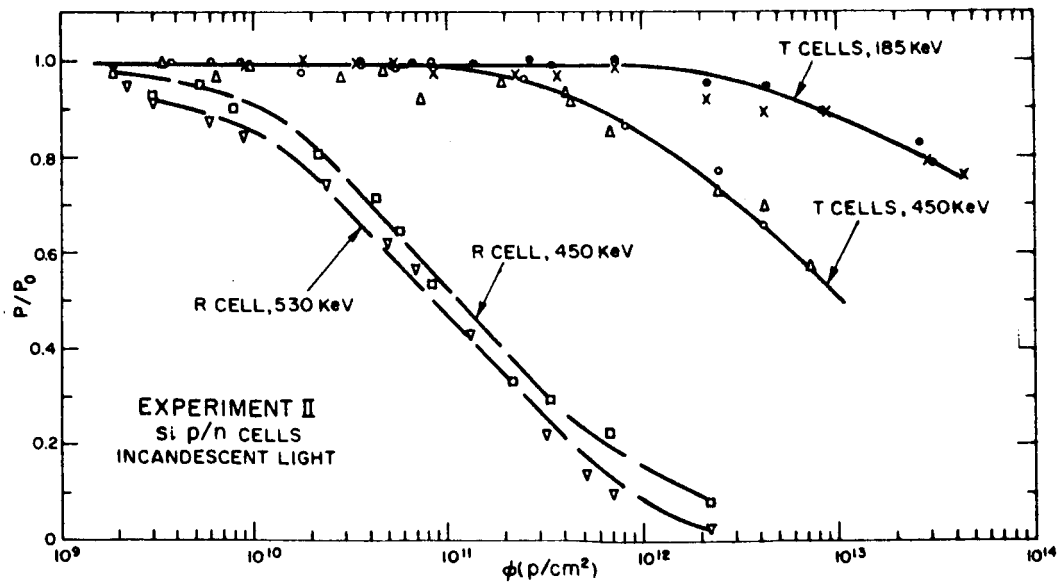

Fig. 5. P/P_o vs. ϕ for Si p/n cells.

protons is approximately 70, signifying that the voltage degradation makes a substantial contribution to the drop in power. This is shown more clearly in Fig. 6 where the current, voltage, and power for cell R-IA are shown. Throughout the flux range, the drop in voltage equals or exceeds that in current. This voltage drop is much more pronounced than has ever been observed in higher-energy irradiations.

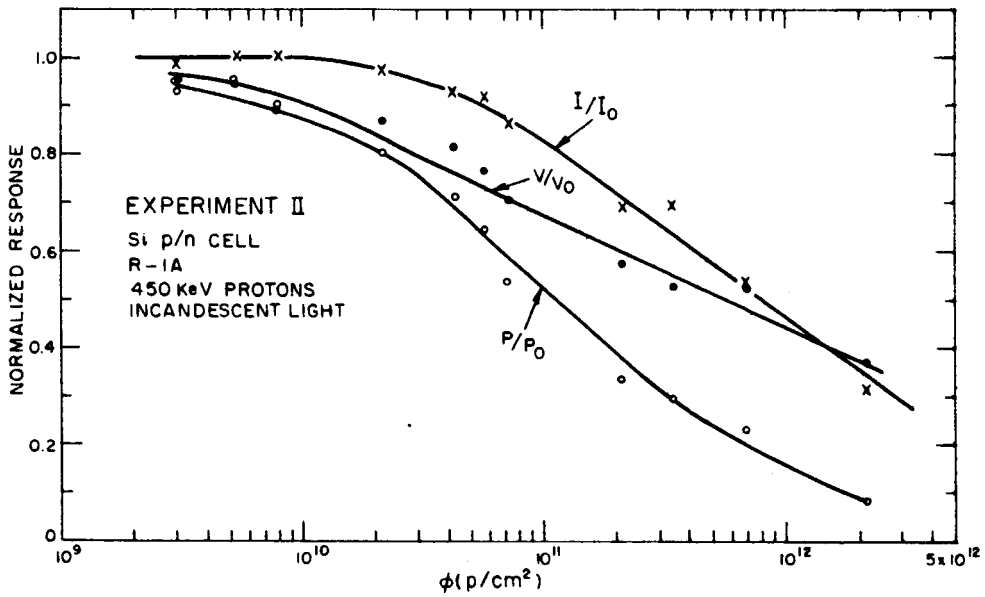

Fig. 6. Normalized response of Si p/n cell vs. flux.

b. Si n/p Cells – The open-circuit voltage vs. flux curves for the Si n/p cells are shown in Fig. 7. In this energy range, the degradation rate increases with proton energy. Accompanying the change in voltage was a "softening" of the photocharacteristic, a result of increasing dark current and series resistance (see below).

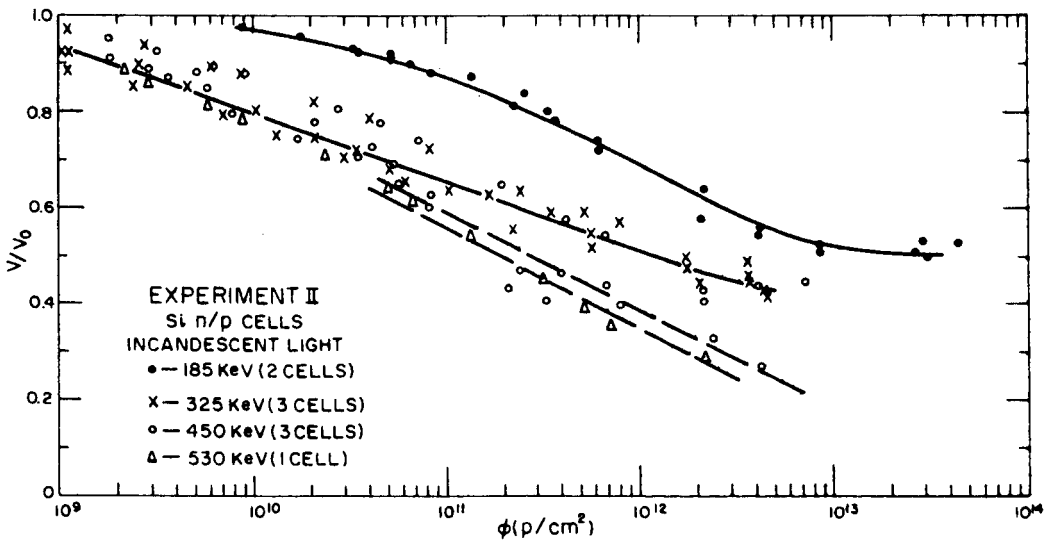

Fig. 7. V/V_o vs. ϕ for Si n/p cells.

The short-circuit current curves are shown in Fig. 8. The shape of these curves is similar to that observed with the p/n cells above. Once degradation commences, the rate of decrease with flux is rapid (~ 50%/decade).

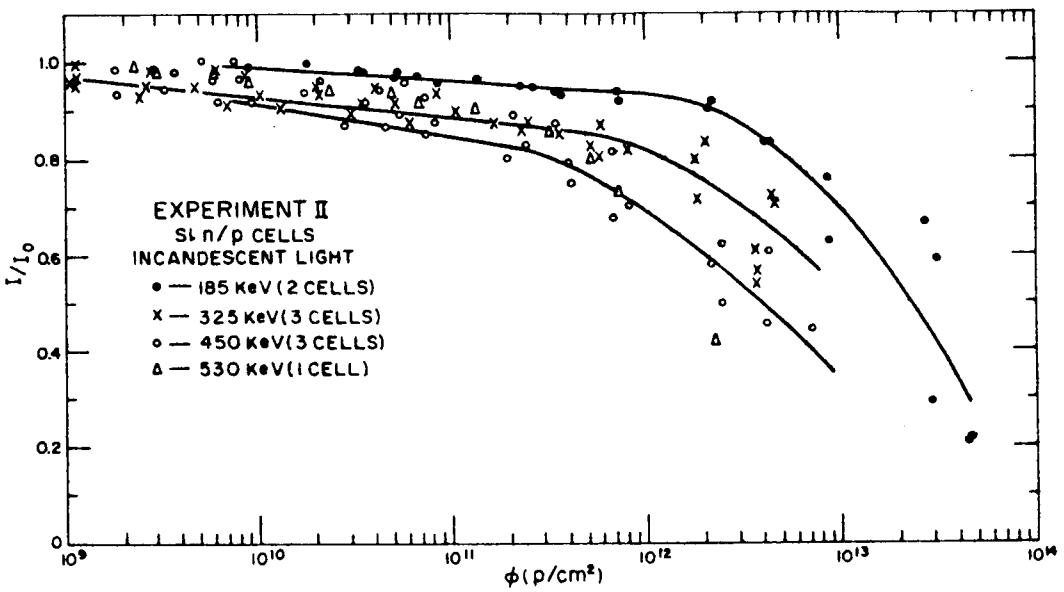

Fig. 8. I/I_o vs. ϕ for Si n/p cells.

The power output curves in Fig. 9 show the same trend as the current and voltage curves do as far as the energy dependence is concerned. However, one cell irradiated with 450-keV

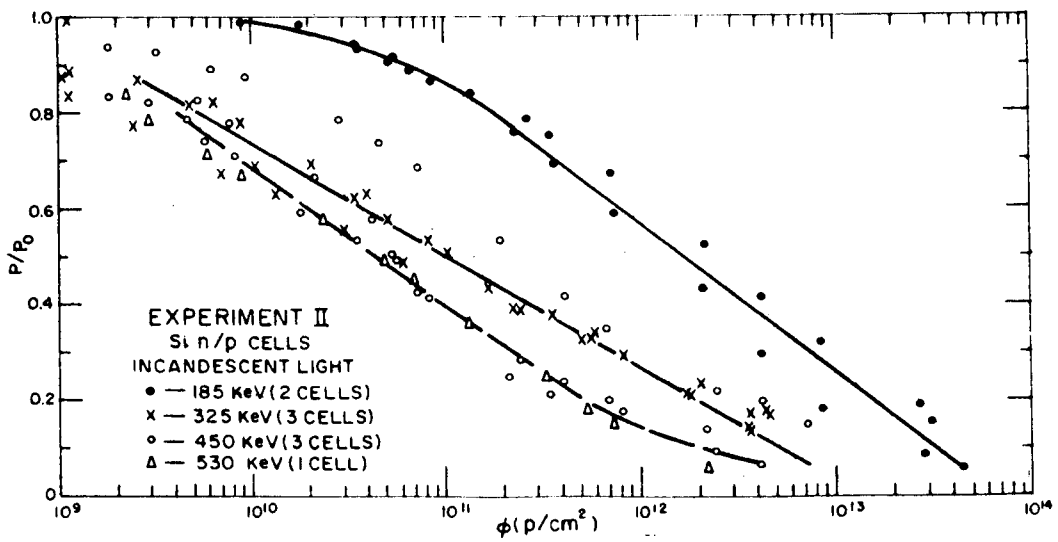

Fig. 9. P/P_o vs. ϕ for Si n/p cells.

protons deviates from this trend. Its power output decreased less than in cells irradiated with 325-keV protons primarily because of a smaller change in voltage during irradiation. The importance of the voltage drop in the change in power is shown in Fig. 10 for a typical cell, MR 9A.

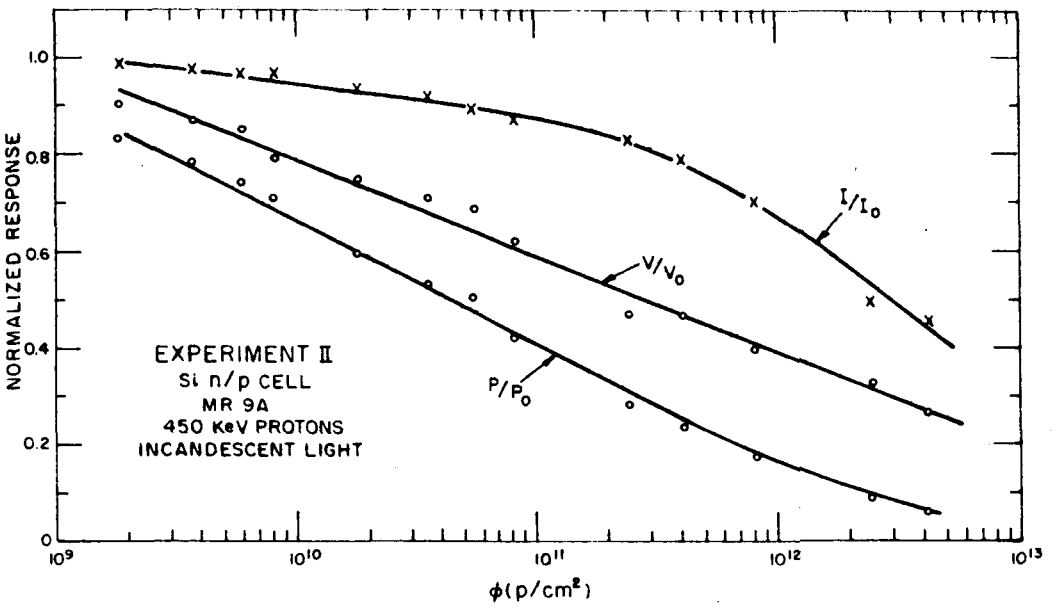

Fig. 10. Normalized response of Si n/p cell vs. flux.

Throughout the flux range, the drop in voltage exceeds that in current, similar to the behavior obtained in the p/n cells.

Considerable scatter is evident in the above figures. Factors contributing to this scatter are slight variations in the junction depth and thickness of the antireflection coating, and possibly in the beam distribution from one run to the next.

c. ***GaAs Cells*** – The change in voltage for the SG and specially treated SCR cells is shown in Fig. 11. No energy dependence is observed for the SG cells while higher energy protons are more damaging for the SCR cells. The anomalous dependence shown for the SCR cells (i.e., 530-keV protons are less damaging than 450-keV protons) is associated with different junction depths and other cell properties. The SCR cells were made from two crystals. The one bombarded with 530-keV protons was cut from crystal lot No. 71. It is seen below that cells made from this lot also showed differences in the current and power output at high fluxes.

The change in current of the specially treated SCR cells is shown in Fig. 12. The damaging ability of the protons increases with proton energy over this range of energies. At any energy, however, the current drops rapidly with flux (~ 35%/ decade). (The 325-and 350-keV data in Fig. 12 apply to cells made from crystal lot No. 71. At fluxes above 10^{11} p/cm^2, the current from these cells degrades more slowly than for the other SCR cells.) Similar comments apply to the data for the SG cells. However, the SCR cells exhibit a larger energy dependence and damage susceptibility than the SC cells.

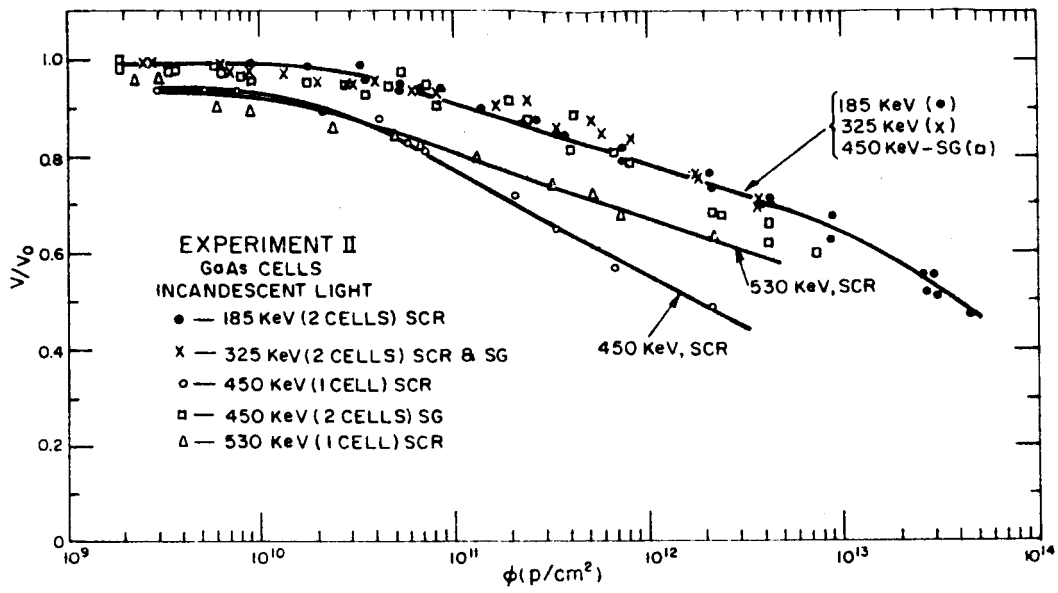

Fig. 11. V/V_o vs. ϕ for GaAs cells.

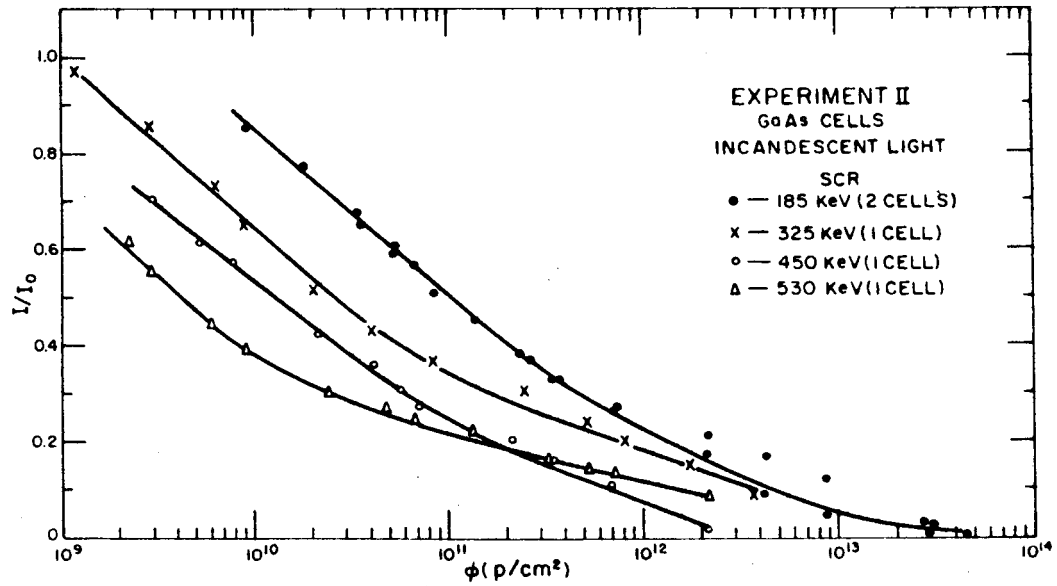

Fig. 12. I/I_o vs. ϕ for GaAs cells.

Power-output curves in the SCR cells are shown in Fig. 13. The drop in power is due almost exclusively to the drop in current. This result is clearly shown in Fig. 14 where the power and current for cell SG92-11A closely follow each other with very little change in open-circuit voltage. This behavior is very different from that observed with the Si cells.

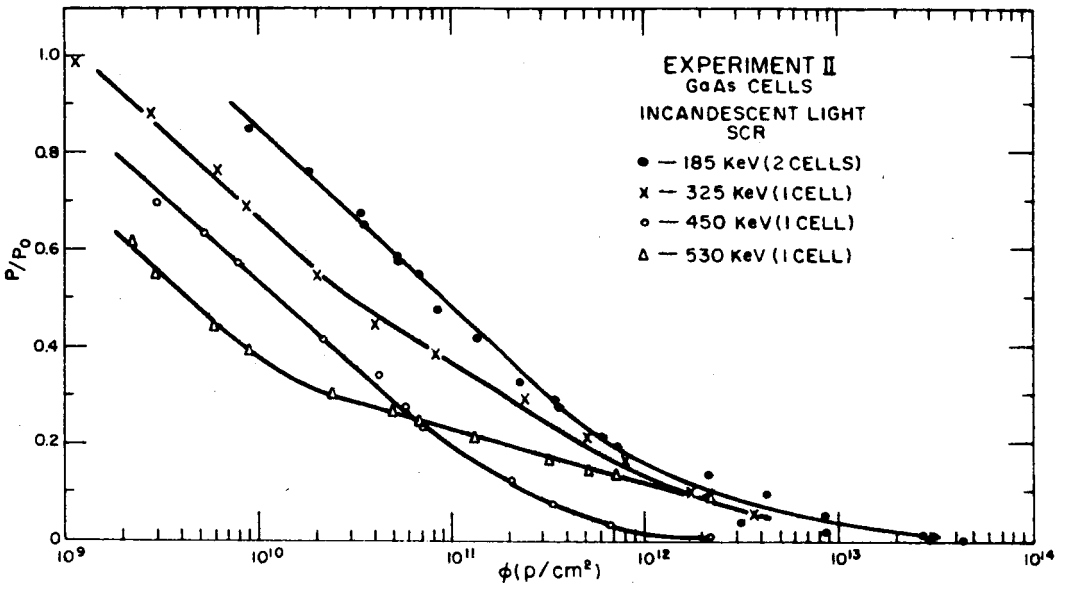

Fig. 13. P/P_o vs. ϕ for GaAs cells.

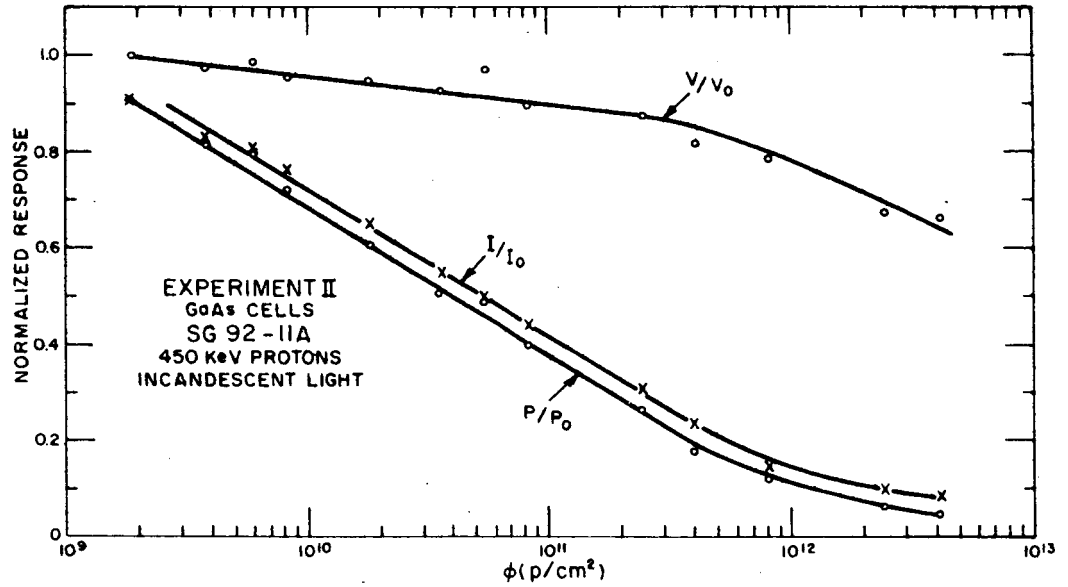

Fig. 14. Normalized response for GaAs cell vs. flux.

d. Critical Fluxes and Sunlight Measurements – Only measurements before and after bombardment were obtained in sunlight on these cells. Consequently, critical flux values ϕ_c, at which the output power drops by 25%, are based on the incandescent light measurements. Table IV lists these values. The IRC-T cells which had a lower efficiency, and presumably a larger junction depth than most of the other cells, are the most radiation-resistant cells. The Hoffman R cells which are comparable in efficiency and junction depth to the Si n/p cells are approximately four times more resistant to damage than the n/p cells. (One Si n/p cell, however,

was as good as the R cell irradiated with 450-keV protons.) Above 185-keV, the Si n/p and GaAs cells have comparable ϕ, while the GaAs SCR cells have the lowest values.

TABLE IV

APPROXIMATE ϕ_c P/cm^2 FOR INCANDESCENT LIGHT

CELL	η_o (%)	PROTON ENERGY (keV)			
		185	325	450	530
Si p/n, T (IRC)	6.5	6.3×10^{13}	–	2.2×10^{12}	–
Si p/n, R (Hoffman)	9.9	–	–	3.1×10^{10}	2.2×10^{10}
Si n/p, MR (RCA)	10.5	2.9×10^{11}	8.8×10^{9}	7.5×10^{9}	6.2×10^{9}
GaAs SG	7.6	–	1×10^{10}	6.2×10^{9}	–
SCR (specially treated)	8.5	1.9×10^{10}	7×10^{9}	2.5×10^{9}	8.6×10^{8}

A comparison of the ratio of the terminal to initial values of current and power was made for the incandescent and sunlight measurements. The GaAs cells were degraded by roughly the same amount for both light sources while the Si cells were only slightly improved in sunlight. This behavior of the Si cells is different from that observed in higher-energy irradiations where sunlight measurements show a smaller degradation than that in incandescent light. An explanation for this behavior can be found in the spectral response measurements. Low-energy protons substantially damage the "blue" response of the Si cells; consequently, the observed degradation is not as sensitive to the light source used as in the case where the "red" response of the cell is primarily reduced.

3. Spectral Response

Spectral response measurements were made on a number of cells, and they demonstrated clearly the effects arising from the small proton range.

The response lost in the Si p/n cells is shown in Fig. 15. The behavior of the Hoffman R cell parallels that of the n/p cells except that the loss in response for the same flux is greater than that for the n/p cell at this energy. For the IRC-T cells, on the other hand, the degradation in response in the "blue" region continues to exceed that in the "red" even at the highest proton energy. This behavior is surprising since the range of 545-keV protons is sufficient to damage regions up to 5 microns (45° irradiations), well into the n-type base. The lifetime in n-type Si is known to degrade more rapidly than in p-type. Consequently, a greater change in the "red" response was expected. Some other parameter, e.g., the junction depth, must be improving the resistance of these cells to low-energy protons.

The response loss in the collection efficiency, i.e., response per proton, of several Si n/p cells as a function of wavelength λ and reciprocal absorption constant α^{-1} is shown in

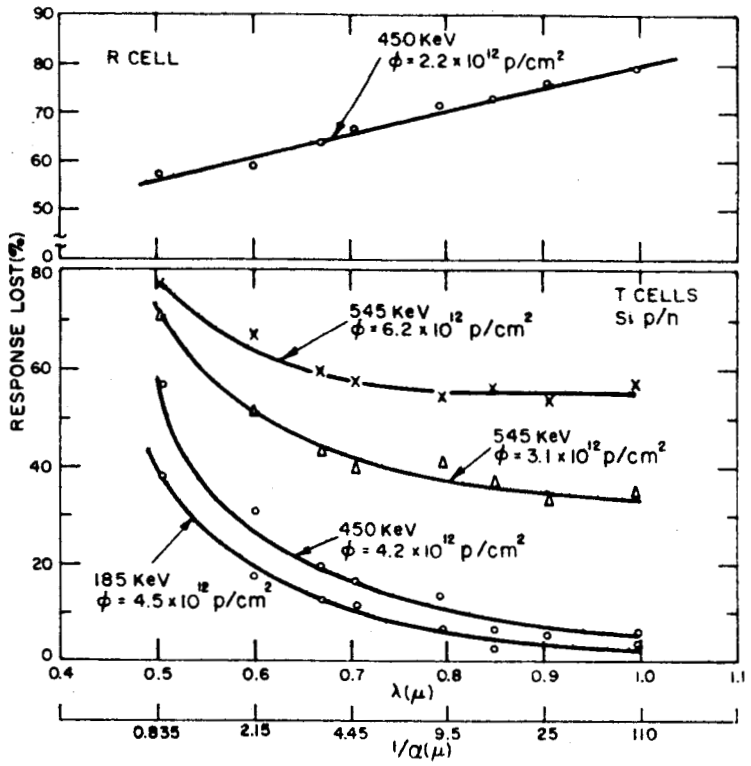

Fig. 15. Percentage spectral response lost vs. λ and $1/\alpha$ for Si p/n cells.

Fig. 16 after bombardment with fluxes of 3.1 to 4.5 × 10^{12} p/cm^2. The 185-keV protons damage primarily the "blue" response (the response arising from surface collection) while 545-keV protons reduce the response at all wavelengths. While the overall response drops with increasing

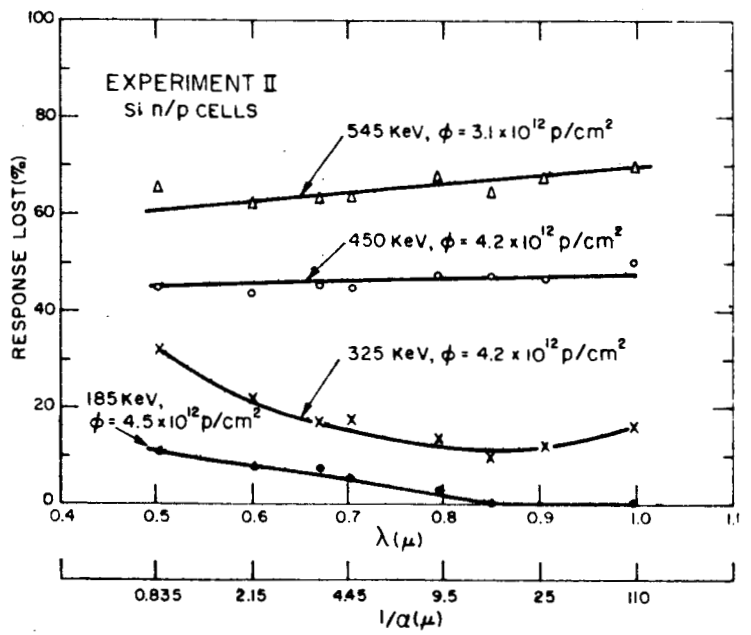

Fig. 16. Percentage spectral response lost vs. λ and $1/\alpha$ for Si n/p cells.

proton energy, the response to red light decreases much faster, eventually surpassing the decrease in "blue" response for proton energies above 325 keV. This behavior is due to the increasing proton range.

The response lost in the GaAs SG and SCR cells is shown in Fig. 17. Bombardment in this case resulted in an appreciable overall drop in response. The drop was the greatest in the

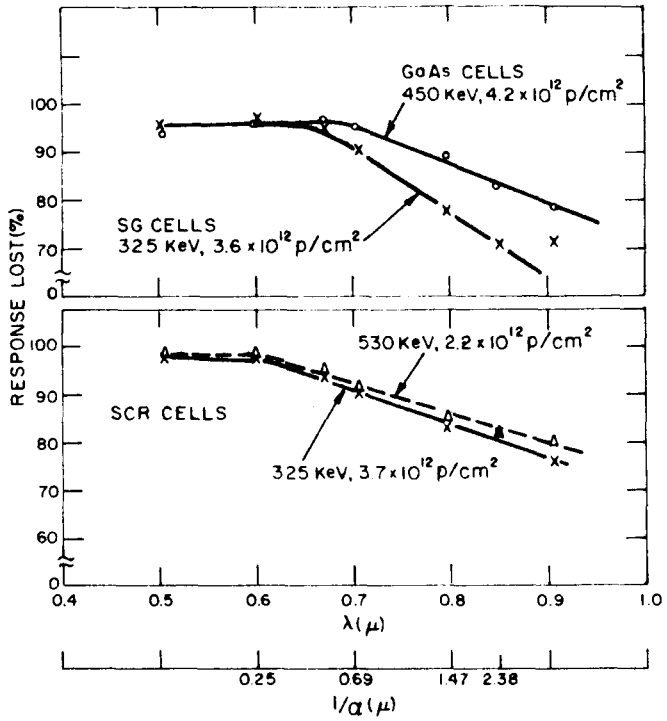

Fig. 17. Percentage spectral response lost vs. λ and $1/\alpha$ for GaAs cells.

"blue" region, tapering off toward the "red". These results are consistent with the fact that the short-circuit current of GaAs cells is due to surface collection of the photogenerated carriers. Short-range particles damage these surface regions reducing the collection efficiency drastically. The reduction in collection efficiency tapers off toward the "red" region where the photocarriers are created closer to the junction and, hence, more efficiently collected.

4. Diffusion Lengths

The sum of the diffusion lengths L on both sides of the junction was measured in several cells before and after bombardment.[19] Each cell was given only one dose of radiation. Results are shown in Fig. 18 where the fractional diffusion length remaining in the Si p/n and n/p cells is plotted against flux. The scatter is quite large. However, it is evident that 185-keV protons produce only a small degradation ($\sim$ 10%) which does not change up to fluxes of 10^{13} p/cm^2.

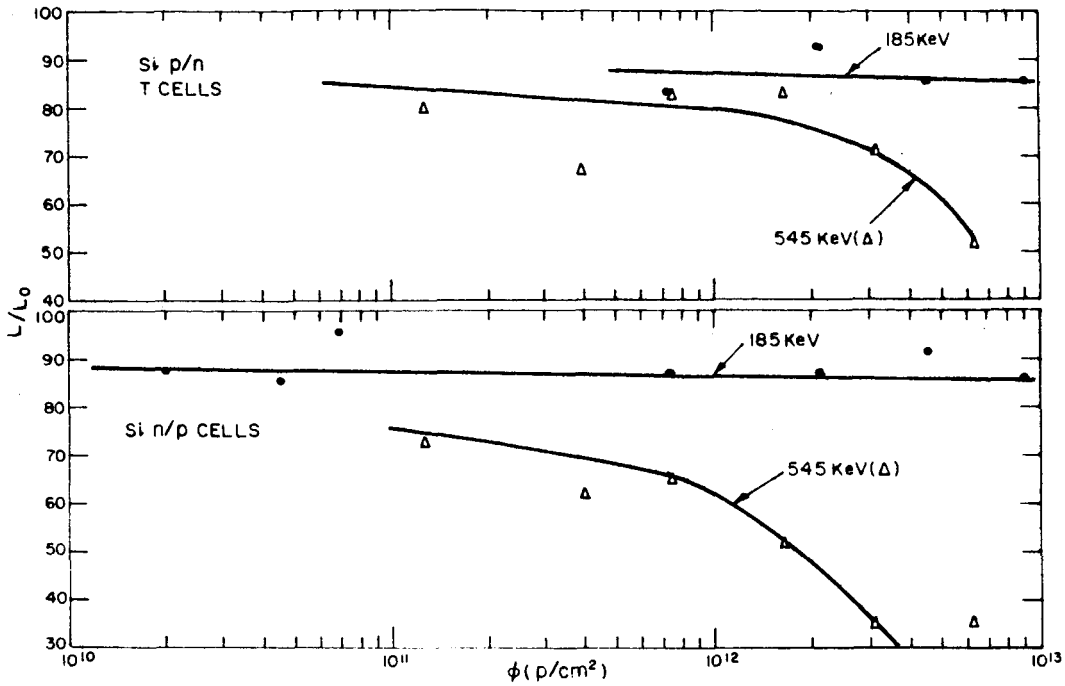

Fig. 18. L/L_o vs. ϕ.

The degradation caused by 545-keV protons on the other hand increases with flux. At a given flux, the degradation is larger in the n/p cells than in the p/n T cells in accord with the spectral response measurements.

Both the spectral response and diffusion length measurements show that the base diffusion length is not reduced to a small value even after an appreciable irradiation. Consequently, the short-circuit current of Si cells would be expected to be resistant to low-energy protons as was found to be the case.

The diffusion lengths in several GaAs cells were also measured, by the electron-voltaic effect, assuming that 3.6 eV is required to produce an electron-hole pair. The fractional diffusion length remaining is compared in Table V with the remaining short-circuit current. The drop in current is much greater than that in L. Since the measured diffusion length is the sum of the skin and base diffusion lengths, the above data are in accord with the fact that GaAs cells depend on regions close to the surface for most of their response. The difference in L before and after bombardment puts an upper limit of about 1 micron for the region from which photogenerated carriers are collected in GaAs.

TABLE V

FRACTIONAL DIFFUSION LENGTH AND SHORT-CIRCUIT CURRENT IN GaAs

PROTON ENERGY (keV)	FLUX	SG			SCR (Specially Treated)		
		L_f/L_o (%)	L_o-L_f (μ)	I_f/I_o (%)	L_f/L_o (%)	L_o-L_f (μ)	I_f/I_o (%)
185	4.5×10^{10}	–	–	–	85	0.24	51
	6.8×10^{10}	86	0.3	69	–	–	–
325	3.6×10^{12}	60	0.9	14	43	0.97	8.2
	4.6×10^{12}	70	0.61	16	–	–	–

5. Comparison with Proton Experiment I

Similar behavior was observed in the degradation of Si and GaAs cells in Experiments I and II. In both experiments, the drop in voltage was a substantial factor in the degradation in the Si cells while the drop in current predominated in the GaAs cells. Although the curve shapes were similar in both experiments, the fluxes at which a given degradation occurred were generally larger in Experiment I than in Experiment II. The factor by which the flux in Experiment I must be reduced to agree with that in Experiment II on the basis of the current degradation is shown in Table VI. The factor based on current is used since the voltage (and power) depend upon the

TABLE VI

FLUX FACTOR BETWEEN EXPERIMENTS I AND II BASED ON INCANDESCENT LIGHT MEASUREMENTS OF CURRENT

ENERGY (keV)	Si p/n T and PH	Si n/p	GaAs G and SG
185	0.3	3	2
545	0.3	10	3

junction properties of the Si cells. Table VI indicates at most an order of magnitude difference in the flux values required for a given change in current. Since the Si n/p cells required more flux for a given change in Experiment II than in Experiment I (the reverse is true for the Si n/p and GaAs cells), some part of the difference must be due to the difference in junction depth of the cells run in Experiments I and II (see Table III). The cells with shallower junctions require less flux for a given drop in current.

The dark I-V characteristics of several cells were measured after bombardment in Experiment I to shed light on the rapid drop in voltage in the Si cells. Pieces of the parent cell which were not bombarded were used for comparison. Typical data are shown in Fig. 19 for a Si n/p cell and in Fig. 20 for a GaAs cell irradiated with 545-keV protons. There is a substantial

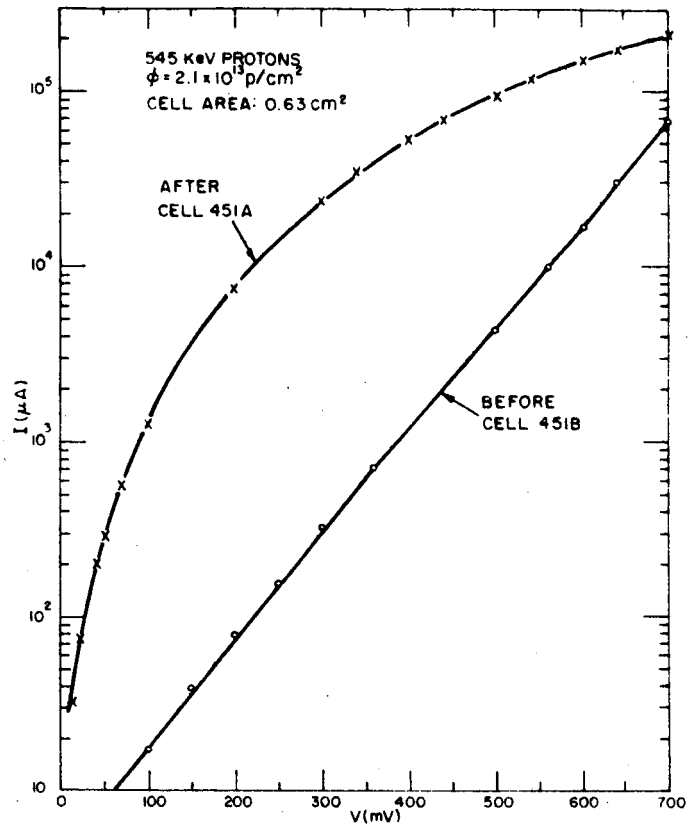

Fig. 19. Forward I-V characteristic of n/p cell.

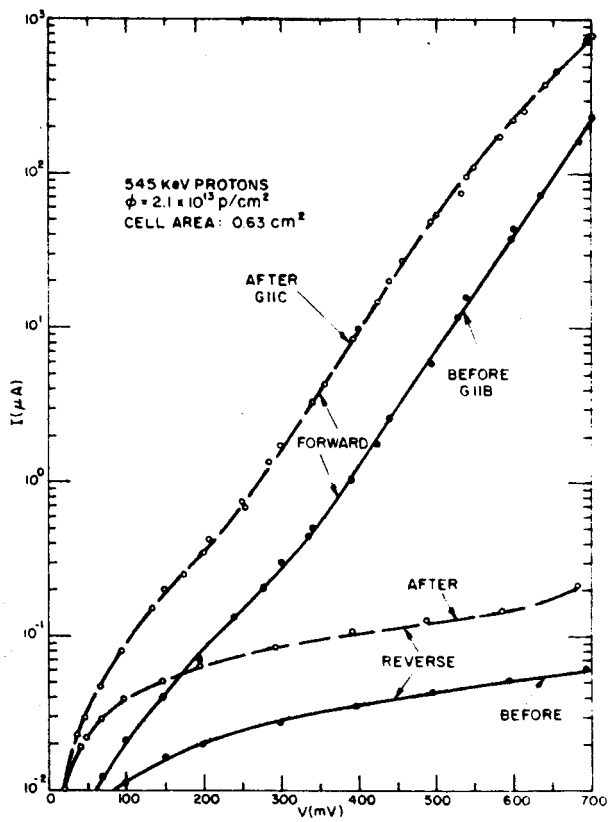

Fig. 20. Forward and reverse characteristic.

increase in the forward current at a given voltage for the Si cell; a much smaller change is observed in the GaAs cell. The increase in forward current necessarily required the open-circuit voltage to decrease. Furthermore, the series resistance in the Si cell has also increased after bombardment, due probably to the introduction of carrier removal sites in the base region adjacent to the junction. The added resistance reduces the rectangularity of the photo-characteristic, leading to a further drop in power output.

C. DISCUSSION OF RESULTS

As expected, the junction depth is an important parameter in low-energy proton irradiation. The scatter observed in the data is partially due to this factor. Furthermore, differences in junction depth complicated the comparison of results from Experiments I and II. Since only a few junctions have been measured at this time, a quantitative treatment of the data cannot be presented. However, qualitative agreement with the idea that the deeper junctions are more damage-resistant has been found.

The range of low-energy protons in GaAs and Si is extremely short. Therefore, only the first few microns of material are damaged. Surface collection of photogenerated carriers and the junction characteristic should be the most seriously affected cell properties. This was demonstrated; GaAs cells suffered a large drop in current since they absorb light and collect carriers from near the surface while the Si cells showed appreciable changes in the junction characteristic and hence open-circuit voltage. The photocurrent of Si cells degraded more slowly than in GaAs since only approximately 20% of this current is due to collection from the shallow-diffused skin.

It was shown that carrier collection from the base region in Si cells is substantial after irradiation, even in the case of 545-keV protons with a range of 5 μ (45° irradiation). This effect is possible since the damaged region in the base is thin and photogenerated carriers from deep in the base can pass through this layer to the junction giving rise to an effective diffusion length larger than that in the damaged region. The behavior to be expected can be obtained from a solution of the continuity equation for a base region consisting of two distinct parts, one with a diffusion length L_1 next to the junction and the other with the initial diffusion length L_2. The extent of the region with a diffusion length L_1 is X_1 where X_1 is the proton range corrected for 45° irradiated minus the sum of the junction depth ℓ and the thickness of the antireflection coating. The continuity equation, excluding fields due to the lifetime gradient,[20] is

$$D \frac{d^2n}{dX^2} - \frac{n}{\tau} = A \qquad (3)$$

where A is the generation rate of carriers in #/cm^3-sec and the other symbols have their customary meaning. Equation (3) is solved for both regions in the base with the following boundary

restrictions. The carrier density n and its gradient are continuous across the boundary separating the two regions in the base. The gradient in carrier density is zero for points deep into the base region. The excess density is zero at the junction.

From this solution, the measured diffusion length L* can be related to L_1, L_2 and X_1 as follows:

$$L^* = \frac{L_1}{(L_1+L_2)e^{X_1/L_1}-(L_1-L_2)e^{-X_1/L_1}} \left\{ (L_1+L_2)e^{X_1/L_1} + (L_1-L_2)e^{-X_1/L_1} + 2\left(\frac{L_2^2-L_1^2}{L_1}\right)\right\} \tag{4}$$

This solution has the proper behavior when $L_1 = L_2$; $L_1 = 0$; X_1 is finite; and $X_1 \to \infty$. The computed behavior is plotted in Fig. 21 where L* is shown vs. the reciprocal value of L_1.

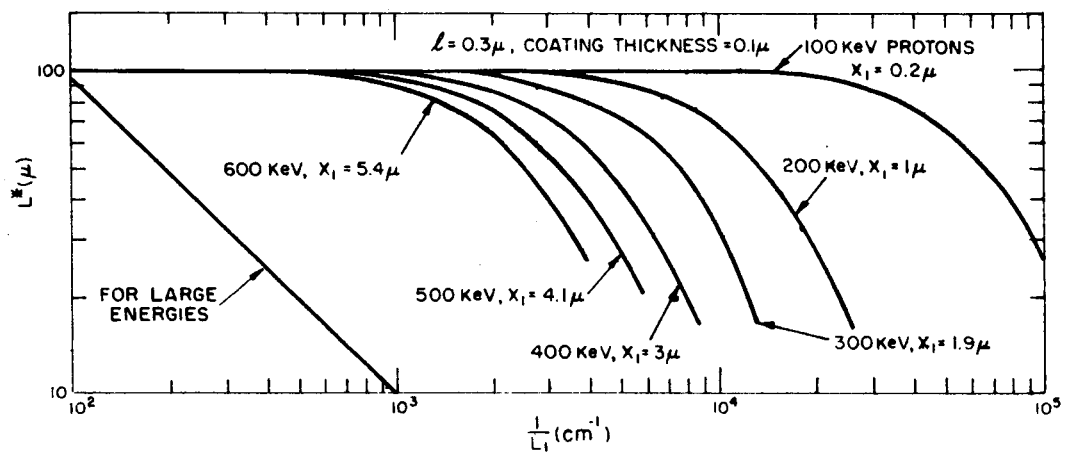

Fig. 21. L* vs. $\frac{1}{L_1}$.

The value used for L_2 was 100 microns. Figure 21 shows that as the proton energy, and hence X_1, increases, the onset of a change in L* occurs at larger values of L_1 and hence smaller values of flux. This behavior is in qualitative agreement with the experimental results and has two ramifications. First, at large fluxes, the current in Si cells is dominated by the low diffusion lengths near the surface. The current degradation should then become similar to that observed in GaAs cells. A rapid drop-off of the current with flux is observed in the Si cells. Secondly, this model predicts the energy dependence of the data. The degradation in cell performance increased with proton energy. Arguments based on the introduction rate of lattice displacements would indicate the opposite trend since the Rutherford scattering cross section varies with the reciprocal particle energy. In low-energy bombardments, however, the overriding factor is the range.

The following argument can be made to compare the theoretical and experimental results. The photovoltaic current is some function of L*, or from Fig. 21, L_1. At high fluxes, L_1 is expected to vary with flux as follows:

$$L_1^2 = \frac{1}{K\phi} \tag{5}$$

Since the damage constant K is expected to vary directly with the lattice-displacement introduction rate $\sigma\nu$, the flux for a given L_1 will vary as

$$\phi \propto \frac{1}{L_1^2 \sigma\nu} \tag{6}$$

With 185-keV protons as a reference, the flux of protons with energy E required for a given degradation in current, i.e., a given value of L*, will be given by

$$\frac{\phi_{185}}{\phi_E} = \frac{(L_1^2 \sigma\nu)\, E}{(L_1^2 \sigma\nu)_{185}}, \quad L^* = \text{constant.} \tag{7}$$

Table VII lists the computed flux ratios for an L* of 50 microns as well as the experimentally determined critical flux ratios. Although the quantitative agreement between the last two columns of Table VII is not perfect, due in no small measure to the fact that the currents were measured with white light, the trend is correctly predicted. Consequently, a damage rate which increases with proton energy can be ascribed to the increasing proton range.

TABLE VII

COMPUTED AND EXPERIMENTAL DEGRADATION RATES

E(keV)	$(L_1)^2_E / (L_1)_{185}$	$(\sigma\nu)_E / (\sigma\nu)_{185}$	$(L_1^2 \nu)_E / (L_1^2 \sigma\nu)_{185}$	ϕ_{c185} / ϕ_{cE} (Si n/p cells experimental)
185	1	1	1	1
325	4.9	0.61	3	4.1
450	15.2	0.46	7	15
545	25	0.39	9.8	15

Although the above argument considered Si cells only, similar results are expected to apply to GaAs. The range of protons in GaAs is roughly half that in Si, but the surface regions are the only active ones in GaAs. Only when the proton range exceeds the thickness of the region in GaAs ($\sim 1\,\mu$) from which carriers are collected, and the introduction rate of lattice displacements ($\sim$ twice as large as in Si) drops further (E > 530 keV), will the superiority of the GaAs-type cell become evident.

The relative superiority of Si n/p and p/n cells is the final item to consider. It has been amply demonstrated that p-type Si is more radiation-resistant than n-type for higher energy protons. If we make the (reasonable) assumption that this is true also for lower proton energies,

then for short-range particles, where most of the damage would take place in the shallow diffused region, p/n cells would be expected to be superior to n/p cells. Our experimental findings are consistent with this. For the lower energy radiation, p/n cells were indeed found to be more damage-resistent. At higher proton energies, increased penetration into the base region resulted in n/p cells becoming more radiation-resistant.

D. CONCLUSIONS

Both GaAs and Si cells deteriorate rapidly as a result of low-energy protons. The major changes which occur are in the junction characteristic and open-circuit voltage in Si cells, and the short-circuit current in GaAs cells.

In general, the behavior of the cells is different from that observed in higher energy irradiations. For example, the damage rate increased with proton energy instead of decreasing as it does with higher-energy protons. The difference in behavior is attributed to the short range of low-energy protons which emphasizes the regions close to the surface of the cell.

PROGRAM FOR NEXT REPORTING INTERVAL

For the EPR work on the new center, the first item will be the firm establishment of the defect introduction rates at energies from 1 to 6.6 MeV. These will require some additional irradiations. Optical absorption measurements will then be made to correlate with the EPR work. Through this program it is hoped to further identify the new defect center and to clearly establish the level in the bandgap to be associated with it.

The effect of impurities on the radiation-damage properties of silicon will be studied using the diffusion length and EPR measurements as described in Section III. Now that proper measurement and fabrication techniques have been worked out for the diffusion length studies, cross-comparisons of surface-barrier and diffused cells made from the same material will be performed as a final check to assure the validity of this approach. Irradiations at 1 MeV will be used to damage the material since complete facilities for this are present at these laboratories. For the EPR work, electron irradiations at 6.6 MeV have been chosen to produce the defects to be studied in sufficient quantities. It is planned to study specifically the effects of different metallic impurities.

REFERENCES

1. G. Feher, Bell System Tech. J. **36**, 449 (1957).
2. J. P. Gordon, Rev. Sci. Inst. **32**, 658 (1961).
3. J. Corbett and G. Watkins, Phys. Rev. Letters **7**, 314 (1961).
4. G. Watkins, Bull. Am. Phys. Soc. **9**, 48 (1964).
5. G. K. Wertheim, J. Appl. Phys. **30**, 1166 (1959).
6. G. Watkins, Disc. Faraday Soc. **31**, 86 (1961).
7. D. Hill, Phys. Rev. **114**, 1414 (1959).
8. V. Vavilov and A. Plotnikov, J. Phys. Soc. Japan **18** Suppl. III, 230 (1963).
9. W. Rosenzweig, Bell System Tech. J. **41**, 1573 (1962).
10. N. J. Hansen, IRE Trans. Nuc. Sci. **NS-9**, 217 (1962).
11. R. C. Waddel, "Radiation Damage Experiments on Relay," Trans. Photovoltaic Specialist's Conf. **1**, (1963).
12. G. W. Longanecker, "Preliminary Results of the Solar Cell Damage Experiment Flown on the Explorer XII Satellite," Proc. Solar Working Group Conf. **1**, (1962).
13. R. E. Fischell, "ANNA 1-B Solar Cell Damage Experience," Trans. Photovoltaic Specialist's Conf. **1**, (1963).
14. J. J. Wysocki, "Radiation Studies on GaAs and Si Devices," IEEE Trans. Nuc. Sci. **NS-10**, 60 (1963).
15. J. W. Freeman, "Detection of an Intense Flux of Low-Energy Protons or Ions Trapped in the Inner Radiation Zone," J. Geophys. Res. **67**, 921 (1962).
16. The only published information on low-energy proton bombardment of solar cells besides that in Ref. 4 can be found in E. Lodi and D. Crowther, Appl. Phys. Letters **2**, 3 (1963).
17. Si ranges – personal communication from J. J. Loferski. The GaAs values were computed by assuming that the range in mg/cm^2 is inversely proportional to the number of electrons per gram of material.
18. P. Rappaport and J. J. Wysocki, "The Photovoltaic Effect in GaAs, CdS and Other Compound Semiconductors," Acta Electronica **5**, 365 (1961).
19. Measured by the technique described by B. McDonald and A. Goetzberger, "Measurement of the Depth of Diffused Layers in Silicon by the Growing Method," J. Electrochem. Soc. **109**, 141 (1962).
20. V. M. Buimistrov, "Theory of the Photodiffusion Effect Caused by a Nonuniform Distribution of Recombination Centers," Soviet Phys. – Solid State **5**, 351 (1963).